

AD-A161 829

(12)

ADP-300677

AD



US ARMY
MATERIEL
COMMAND

20000801190

TECHNICAL REPORT BRL-TR-2684

THE HUGONIOTS OF M-30 PROPELLANT AND AN INERT SIMULATOR OF M-30

Vincent M. Boyle

October 1985

DTIC
SELECTED
NOV 26 1985
S D

APPROVED FOR PUBLIC RELEASE; DISTRIBUTION UNLIMITED.

US ARMY BALLISTIC RESEARCH LABORATORY
ABERDEEN PROVING GROUND, MARYLAND

Reproduced From
Best Available Copy

Destroy this report when it is no longer needed.
Do not return it to the originator.

Additional copies of this report may be obtained
from the National Technical Information Service,
U. S. Department of Commerce, Springfield, Virginia
22161.

The findings in this report are not to be construed as an official
Department of the Army position, unless so designated by other
authorized documents.

The use of trade names or manufacturers' names in this report
does not constitute indorsement of any commercial product.

UNCLASSIFIED

SECURITY CLASSIFICATION OF THIS PAGE (When Data Entered)

REPORT DOCUMENTATION PAGE		READ INSTRUCTIONS BEFORE COMPLETING FORM
1. REPORT NUMBER Technical Report BRL-TR-2684	2. GOVT ACCESSION NO. AD-A161829	3. RECIPIENT'S CATALOG NUMBER
4. TITLE (and Subtitle) THE HUGONIOTS OF M-30 PROPELLANT AND AN INERT SIMULATOR OF M-30	5. TYPE OF REPORT & PERIOD COVERED Final	
7. AUTHOR(s) Vincent M. Boyle	6. PERFORMING ORG. REPORT NUMBER	
9. PERFORMING ORGANIZATION NAME AND ADDRESS US Army Ballistic Research Laboratory ATTN: SLCBR-TB Aberdeen Proving Ground, MD 21005-5066	8. CONTRACT OR GRANT NUMBER(s) 1L162618AH80	
11. CONTROLLING OFFICE NAME AND ADDRESS US Army Ballistic Research Laboratory ATTN: SLCBR-DD-T Aberdeen Proving Ground, MD 21005-5066	10. PROGRAM ELEMENT, PROJECT, TASK AREA & WORK UNIT NUMBERS	
14. MONITORING AGENCY NAME & ADDRESS (if different from Controlling Office)	12. REPORT DATE October 1985	
	13. NUMBER OF PAGES 26	
	15. SECURITY CLASS. (of this report) UNCLASSIFIED	
	15a. DECLASSIFICATION DOWNGRADING SCHEDULE	
16. DISTRIBUTION STATEMENT (of this Report) Approved for public release; distribution is unlimited.		
17. DISTRIBUTION STATEMENT (of the abstract entered in Block 20, if different from Report)		
18. SUPPLEMENTARY NOTES		
19. KEY WORDS (Continue on reverse side if necessary and identify by block number) Hugoniot, M-30 Propellant, Porous Hugoniot		
20. ABSTRACT (Continue on reverse side if necessary and identify by block number) The Hugoniot of M-30 and an inert simulator of M-30 have been determined by shock velocity measurements in samples of these materials. Also, porous Hugoniot for both materials were calculated using the solid Hugoniot and the Mie-Gruneisen equation. A knowledge of the porous Hugoniot is important in predicting the response of a propellant bed to a shock wave.		

DD FORM 1473

1 JAN 73 EDITION OF 1 NOV 65 IS OBSOLETE

UNCLASSIFIED

SECURITY CLASSIFICATION OF THIS PAGE (When Data Entered)

TABLE OF CONTENTS

	PAGE
LIST OF ILLUSTRATIONS	5
LIST OF TABLES	7
I. INTRODUCTION	9
II. SAMPLE PREPARATION	9
A. M-30 Propellant	9
B. Inert Simulator	9
III. PROCEDURE	11
IV. RESULTS	14
V. DISCUSSION	22
REFERENCES	23
LIST OF SYMBOLS	25
DISTRIBUTION LIST	27

RE: Distribution Unlimited
 Distribution Statement A is correct for this report. No information in the report is damaging in the public domain.
 Per Mr. Vincent M. Boyle, ABRL/SLCGR-TB

Accession For	
NTIS CRA&I	↓
DTIC TAB	<input type="checkbox"/>
Unannounced	<input type="checkbox"/>
Justification _____	
By _____	
Distribution/ _____	
Availability Codes	
Dist	Avail and/or Special
A-1	



LIST OF ILLUSTRATIONS

FIGURE	PAGE
1. Initial Configuration of the M-30 Propellant Grain	10
2. Experimental Arrangement Used to Determine the Shock Velocity in the Sample	12
3A. Graphical Interpretation of the Interface Equation for Reacting and Non-Reacting M-30	13
3B. Graphical Interpretation of the Impedance-Matching Technique Reacting and Non-Reacting M-30	13
4. Geometrical Interpretation of Equations (1), (2), and (3)	17
5. A Comparison of the Solid and Porous Hugoniot in the Pressure-Particle Velocity Plane	21

LIST OF TABLES

TABLE	PAGE
1. M-30 Data	14
2. M-30 Inert Simulator Data	15
3. Gruneisen Gamma	16
4. Porous Inert Hugoniot Calculations	19
5. Porous M-30 Hugoniot Calculations	20

I. INTRODUCTION

There was a need for the equation of state of porous propellant so that code calculations could be made to predict the response of propellant beds to shock pressures of varying intensity and duration.

The work reported here is related to the XM1 Compartmentalization Study. One threat to crew and tank is propellant initiation caused by shaped charge jet penetration. What shock pressure conditions will be produced in the propellant bed during shaped charge penetration? Will the propellant reaction under these conditions be so violent that quick venting is not possible? In order to answer these questions, it is helpful to know the shock Hugoniot of the impacted material. The work reported here was specifically directed toward the measurement of the shock Hugoniot for live and inert propellants and calculation of the shock Hugoniot of porous beds of these materials. The live propellant material is the seven perforation M-30 propellant which is used in the 105-mm APDS and HEAT rounds. The inert propellant consists of a thermoplastic material which has been extruded to the same configuration as the live propellant and has approximately the same density. The porous Hugoniot were calculated from the solid Hugoniot using the Mie-Gruneisen equation.

II. SAMPLE PREPARATION

A. M-30 Propellant

The propellant comes in the form of a grain approximately 1.59 cm long, 0.71 cm diameter with seven cylindrical perforations 0.08 cm diameter within the grain, parallel to the long axis, as shown in Figure 1. Samples approximately 0.32 cm long were machined from several propellant grains and carefully sanded and measured for thickness. The small sample thickness was necessitated by the small diameter of the propellant and the need to make a shock velocity measurement through the sample before rarefactions originating at the sample diameter boundary can influence the shock wave. The perforations were filled in with modeling clay in order to prevent jetting and eliminate rarefaction effects on the shock wave in the sample. The clay had a density of 1.65 gm/cm^3 ; the propellant density was 1.66 gm/cm^3 . M-30 is a tripe base propellant which has the following ingredients:

nitrocellulose	28.0 %
nitroglycerine	22.5 %
nitroguanadine	47.7 %
ethyl centralite	1.5 %
cryolite	0.3 %

B. Inert Simulator

The inert simulator is an extruded thermoplastic made by Radford Army Ammunition Plant and it was made to simulate the density of M-30 propellant. It consists of the following:

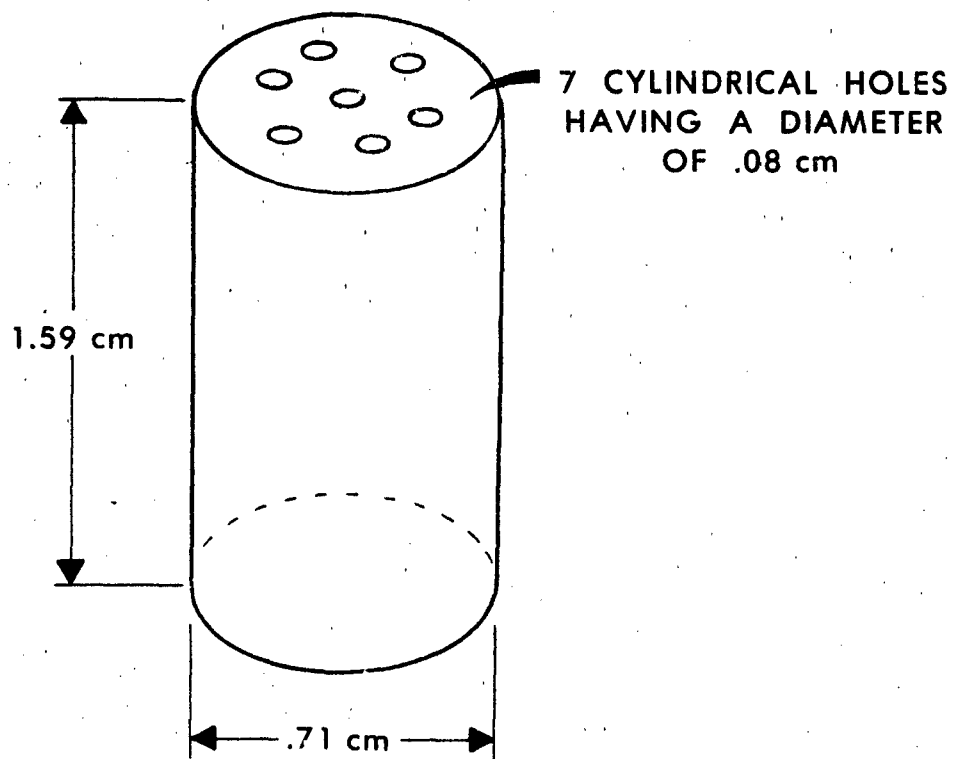


Figure 1. Initial Configuration of the M-30 Propellant Grain.

cellulose acetate	64.2 %
triacetin (plasticizer)	15.0 %
graphite	2.4 %
red lead (Pb_3O_4)	18.4 %

The inert simulator has a density of 1.55 gm/cm^3 . It comes in the form of pellets having approximately the same dimensions and configuration as the live propellant. In order to obtain uniform samples suitable for our measurements the inert was heated to 100°C and compressed in a metallurgical press at 10,000 psi to get a solid cylinder 3.18 cm diameter by 3.81 cm high. Samples .95 cm thick were machined from this and measured for thickness.

III. PROCEDURE

The impedance matching technique¹ was used to determine the solid Hugoniot for the live and inert propellant materials. We used a 10.16 cm diameter plane wave lens, a 2.54 cm thick TNT pad, and various buffer plates to provide a range of known pressures in the buffer plate. The sample of known thickness was placed on the buffer plate and front lighted by an argon bomb light source. The transit time of the shock through the sample was recorded by a Beckman and Whitley Model #770 streak camera writing at 16mm/s, and a shock velocity in the sample calculated. The impedance matching technique was used to calculate the corresponding pressure and particle velocity in the sample. This is illustrated in Figure 2.

Since it was anticipated that the M-30 propellant might react during these measurements, an additional pressure monitor (a Plexiglas pellet) was placed on the propellant free surface. The shock velocity in the Plexiglas pellet was measured and a pressure in the propellant was calculated by using the interface equation. This pressure determination in conjunction with that obtained using the impedance matching technique was used to insure that only unreacted data points would be accepted to calculate the Hugoniot.²

If the propellant were to react it would produce a higher pressure in the Plexiglas overlay than would unreacted M-30. When the interface equation is used, the computed particle velocity in M-30 would be high due to reaction as illustrated in Figure 3A. On the other hand, the particle velocity calculated by the impedance matching technique will be low if the M-30 reacts sufficiently to increase the shock velocity in the sample.

This can be seen by referring to Figure 3B where the particle velocity is determined by the intersection of the buffer plate release adiabat with a line having a slope of $\rho_0 U_s$ where ρ_0 is the initial density of M-30 and U_s is the shock velocity through the sample. Thus a deviation between the particle

¹ Rice, McQueen, Walsh, "Compression of Solids by Strong Shock Waves," Solid State Physics, Volume 6, 1958.

² Boyle, Smothers, Ervin, "The Shock Hugoniot of Unreacted Explosives," Fifth Symposium on Detonation, August 18 - 21, 1970.

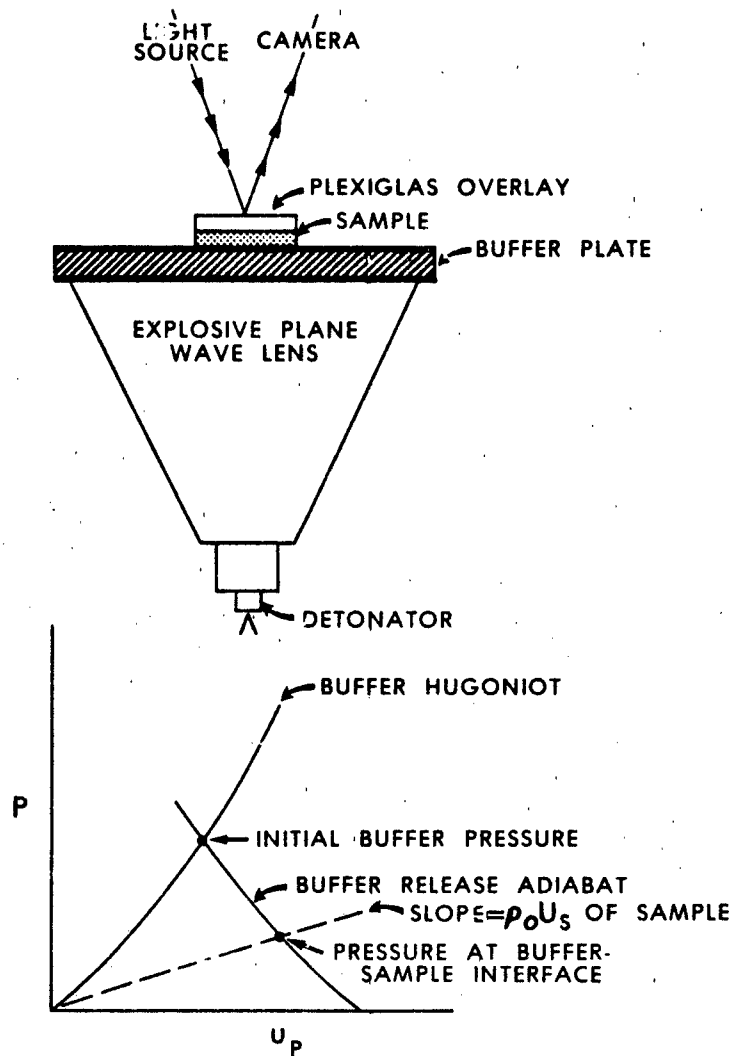


Figure 2. Experimental Arrangement Used to Determine the Shock Velocity in the Sample. Also, shown is a graphical illustration of the impedance-matching technique which was used to calculate the pressure and particle velocity in the sample.

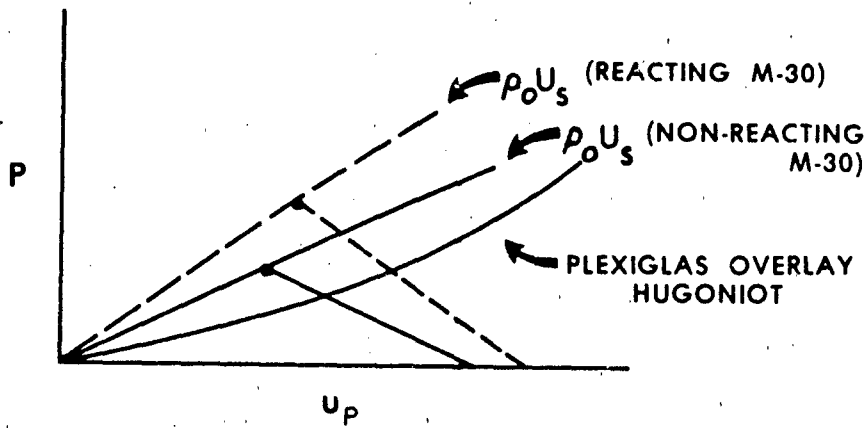


Figure 3A. Graphical Interpretation of the Interface Equation for Reacting and Non-Reacting M-30.

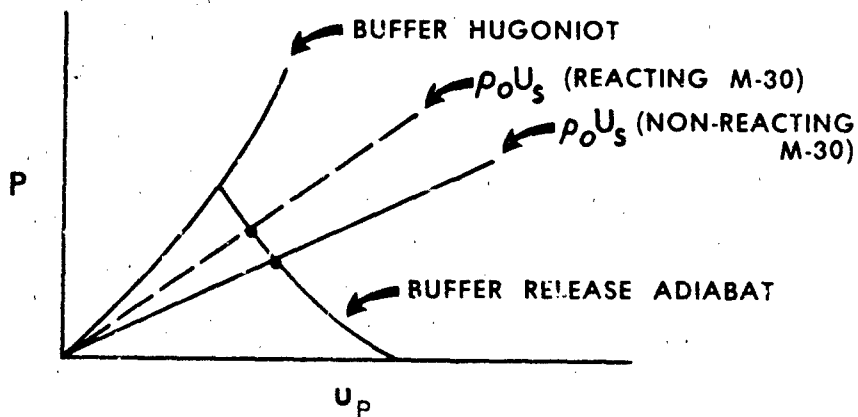


Figure 3B. Graphical Interpretation of the Impedance-Matching Technique for Reacting and Non-Reacting M-30.

velocity calculated at the buffer-M-30 interface and that calculated at the Plexiglas - M-30 interface indicates reaction. Additional information is given in reference 2.

IV. RESULTS

The measured data points for M-30 propellant are shown in Table 1. The numbers in parentheses are data points determined using a Plexiglas overlay and the interface equation to determine particle velocity in the propellant. This was done to see if propellant reaction was affecting the data during the time of measurement (less than one microsecond). The first four lines of data showed little or no reaction and these eight points were used to determine the unreacted Hugoniot for solid M-30 propellant. A least squares fit of the form, $U_s = b + su_p$ gave

$$U_s = 2.661 \times 10^5 + 1.655 u_p \text{ cm/s.}$$

The measured data points for the M-30 inert simulator are given in Table 2. A least squares fit to these data points gave the following Hugoniot for the solid inert simulator.

$$U_s = 2.251 \times 10^5 + 1.509 u_p \text{ cm/s}$$

Table 1. M-30 Data.

ρ_0 (gm/cm ³)	U_s (cm/s)	u_p (cm/sec)	P (Kbars)*	Comments
1.65	3.515×10^5	.508 (.542) $\times 10^5$	29.6 (31.6)	
1.65	4.403×10^5	1.032 (1.081) $\times 10^5$	75.4 (79.0)	
1.66	4.426×10^5	1.031 (1.017) $\times 10^5$	75.8 (74.7)	
1.66	4.391×10^5	1.032 (1.118) $\times 10^5$	75.3 (81.5)	
1.66	5.248×10^5	1.464 (2.415) $\times 10^5$	127.5 (210.4)	Reaction
1.66	5.226×10^5	1.465 (2.258) $\times 10^5$	127.1 (195.9)	Reaction
1.66	5.476×10^5	1.445 (2.622) $\times 10^5$	131.3 (226.1)	Reaction

* 1 Kiloobar = 10^9 dynes/cm²

Table 2. M-30 Inert Simulator Data.

ρ_{0s} (gm/cm ³)	U_s (cm/s)	u_p (cm/sec)	P (Kbars)*
1.55	3.050×10^5	$.522 \times 10^5$	24.7
1.55	3.051×10^5	$.522 \times 10^5$	24.7
1.55	3.863×10^5	1.064×10^5	63.7
1.55	3.804×10^5	1.066×10^5	62.9
1.55	4.611×10^5	1.548×10^5	110.6
1.55	4.592×10^5	1.550×10^5	110.3

* 1 Kiloobar = 10^9 dynes/cm²

The porous Hugoniots^{3 4 5 6} were calculated from the solid Hugoniots using the Mie-Gruneisen equation with a Gruneisen gamma,

$G = V \left(\frac{\partial P}{\partial E} \right)_V$ calculated from thermodynamic properties of the

material at standard temperature and pressure. At standard conditions, the Gruneisen gamma, $G = aC_0^2/C_p$ where a is the volume coefficient of thermal expansion, C_0 is the bulk sound velocity and C_p is the specific heat.

These quantities are shown in Table III. The volume coefficient of thermal expansion for M-30 was assumed to be

$3 \times 10^{-4} \frac{cc}{cc \cdot ^\circ C}$. This agrees well with the values cited in the literature and is probably a good approximation. We assumed the same

value for the inert simulator. The bulk sound velocity was obtained from the unreacted Hugoniot of the solid at zero particle velocity. The specific heat of M-30 was taken from the literature. The specific heat of the inert M-30 simulator was measured by Leon Decker, BRL, using differential scanning calorimetry.

³Herrmann W., "Constitutive Equation for the Dynamic Compaction of Ductile Porous Materials," JAP, Vol. 40, No. 6, May 1969.

⁴Hoffman, Andrews, Maxwell, "Computed Shock Response of Porous Aluminum," JAP, Vol. 39, No. 10, Sept. 1968.

⁵Erkman, Edwards, "Computed and Experimental Hugoniots for Unreacted Porous High Explosives," Sixth Symposium on Detonation, Aug. 24 - 27, 1976.

⁶Zeldovich, Raizer. "Physics of Shock Waves and High Temperature Hydrodynamic Phenomena," Vol. II, Academic Press, New York, 1967.

Table 3. Gruneisen Gamma.

Material	a $\frac{\text{cc}}{\text{cc} \cdot ^\circ\text{C}}$	C ₀ (cm/sec)	C _p $\frac{\text{ergs}}{\text{gm} \cdot ^\circ\text{C}}$	G
M30	3×10^{-4}	2.661×10^5	1.502×10^7	1.412
Inert	3×10^{-4}	2.251×10^5	1.247×10^7	1.219

The porous Hugoniot's were calculated using the following simplifying assumptions:

1. G remains constant at its zero pressure value over the range of interest.
2. The zero pressure specific internal energy of the solid and porous material are equal.
3. The materials possess zero strength.
4. Mechanical equilibrium has been established.
5. Thermal equilibrium has been established. Refer to the Discussion Section for more on assumptions 4 and 5.

The Mie-Gruneisen equation of state relates the thermal component of pressure to the thermal component of specific internal energy at a given volume. This can be expressed by the following equation:

$$(P_f - P_s) = \frac{G}{V} (E_f - E_s) \quad (1)$$

where the subscript f refers to the porous material and the subscript s refers to the solid material. The validity of this equation is treated in references 3, 4, 5 and 6.

Using the Rankine-Hugoniot energy equation for the porous and the solid materials the following equations can be written;

$$E_f - E_{of} = 1/2 P_f (V_{of} - V) \quad (2)$$

$$E_s - E_{os} = 1/2 P_s (V_{os} - V) \quad (3)$$

Refer to Figure 4 for a geometrical interpretation of equations (1), (2), and (3). Since we assumed $E_{of} = E_{os}$ equations (1), (2), and (3) can be combined to give:

$$P_f = P_s \left(\frac{V_{os} - V - \frac{2V}{G}}{V_{os} - V - \frac{2V}{G}} \right) \quad (4)$$

Since the Hugoniot of the solid material has been determined experimentally ($U_s = b + su_p$), we can use this relationship and the equations for conservation of mass and momentum across the shock wave to derive an expression for P_s , the shock pressure in the solid material,

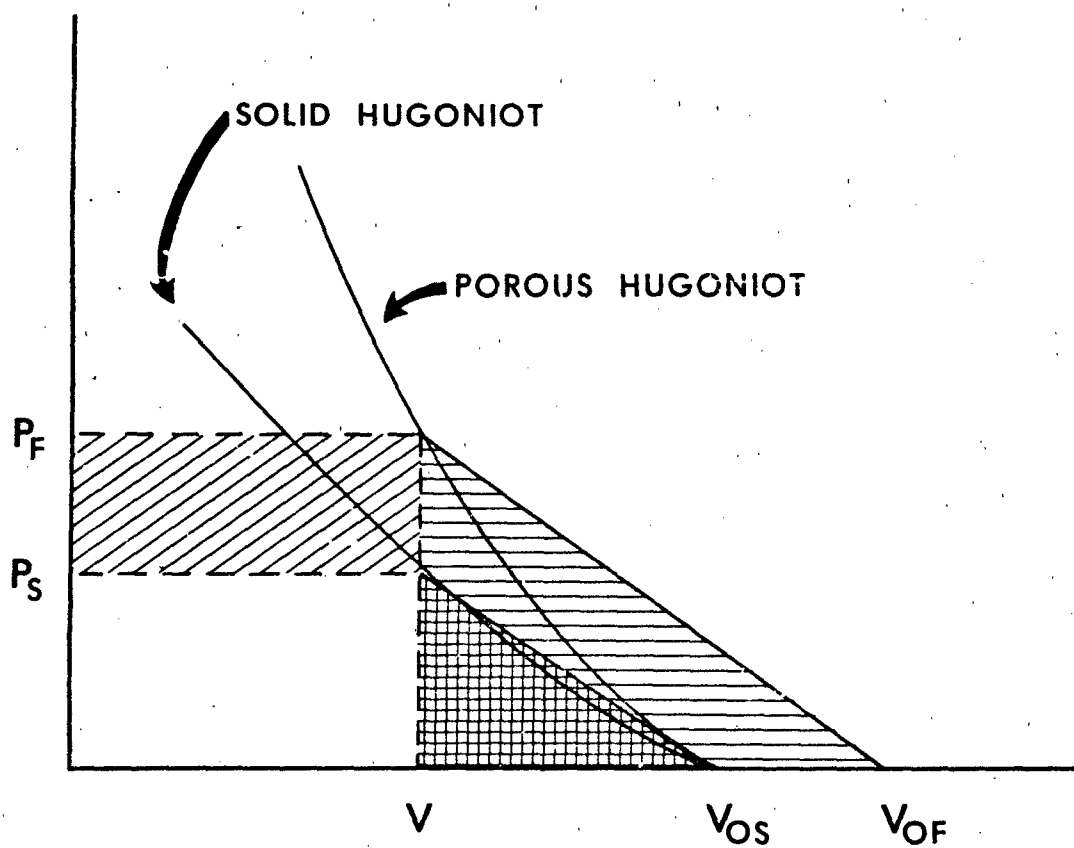


Figure 4. Geometrical Interpretation of Equations (1), (2), and (3).

$$(P_f - P_s) \frac{V}{G} = \frac{1}{2} P_f (V_{of} - V) - \frac{1}{2} P_s (V_{os} - V) .$$

$$P_s = \frac{b^2 (V_{os} - V)}{[V_{os} - s(V_{os} - V)]^2} \quad (5)$$

Equation (4) can then be rewritten,

$$P_f = \frac{b^2 (V_{os} - V)}{[V_{os} - s(V_{os} - V)]^2} \left(\frac{V_{os} - V - \frac{2V}{G}}{V_{of} - V - \frac{2V}{G}} \right) \text{ kbars} \quad (6)$$

P_f , the pressure in the porous material, is then calculated by substituting values for V , the specific volume of the shocked material, into Equation (6). P_f will be in kilobars for V in cm^3/gm and b in cm/s . Conservation of mass across the shock front requires

$$\frac{U_{sf}}{V_{of}} = \frac{U_{sf} - u_{of}}{V} \quad (7)$$

Conservation of momentum requires

$$P_f - P_{of} = \frac{U_{sf} u_{pf}}{V_{of}} \quad (8)$$

Simultaneous solution of equations (7) and (8) gives

$$U_{sf} = V_{of} \left(\frac{P_f - P_{of}}{V_{of} - V} \right)^{1/2} \quad (9)$$

$$u_{pf} = \left[(P_f - P_{of}) (V_{of} - V) \right]^{1/2} \quad (10)$$

The porous Hugoniot values calculated using equations 6, 9, and 10 are shown in Tables 4 and 5.

Table 4. Porous Inert Hugoniot Calculations.

G	V_{of} (cm^3/gm)	V (cm^3/gm)	P_f (Kbar)	U_{sf} (cm/s)	u_{pf} (cm/sec)
1.216	1.250	.63	4.9	1.109×10^5	$.550 \times 10^5$
1.216	1.250	.62	8.8	1.481×10^5	$.747 \times 10^5$
1.216	1.250	.61	13.6	1.821×10^5	$.932 \times 10^5$
1.216	1.250	.60	19.3	2.152×10^5	1.119×10^5
1.216	1.250	.59	26.2	2.490×10^5	1.315×10^5
1.216	1.250	.58	34.7	2.844×10^5	1.525×10^5
1.216	1.250	.57	45.3	3.226×10^5	1.755×10^5
1.216	1.250	.56	58.8	3.648×10^5	2.014×10^5
1.216	1.250	.55	76.2	4.125×10^5	2.310×10^5
1.216	1.250	.54	99.6	4.681×10^5	2.659×10^5
1.216	1.250	.53	131.9	5.351×10^5	3.082×10^5
1.216	1.250	.52	179.2	6.193×10^5	3.617×10^5
1.216	1.250	.51	253.6	7.137×10^5	4.332×10^5
1.216	1.250	.50	385.5	8.961×10^5	5.337×10^5

A least squares fit of the shock and particle velocities shown above gives the porous inert Hugoniot.

Table 5. Porous M-30 Hugoniot Calculations.

G	V_{of} (cm^3/gm)	V (cm^3/gm)	P_f (Kbar)	U_{sf} (cm/s)	u_{pf} (cm/s)
1.412	1.149	.59	7.7	1.351×10^5	$.658 \times 10^5$
1.412	1.149	.58	15.7	1.911×10^5	$.947 \times 10^5$
1.412	1.149	.57	25.9	2.431×10^5	1.225×10^5
1.412	1.149	.56	39.1	2.959×10^5	1.517×10^5
1.412	1.149	.55	56.5	3.528×10^5	1.839×10^5
1.412	1.149	.54	80.2	4.169×10^5	2.210×10^5
1.412	1.149	.53	113.8	4.926×10^5	2.654×10^5
1.412	1.149	.52	164.1	5.869×10^5	3.214×10^5
1.412	1.149	.51	245.9	7.129×10^5	3.966×10^5
1.412	1.149	.50	398.7	9.006×10^5	5.088×10^5

A least squares fit of the shock and particle velocities shown above gives the porous M-30 Hugoniot.

The Hugoniot of porous M-30 (bulk density = $.870 \text{ gm/cm}^3$) is represented by:

$$U_{sf} = .318 \times 10^5 + 1.720 u_{pf} \text{ cm/s.}$$

The Hugoniot of the porous inert (bulk density = $.800 \text{ gm/cm}^3$) is represented by:

$$U_{sf} = .337 \times 10^5 + 1.617 u_{pf} \text{ cm/sec.}$$

These equations are least squares fits to the calculated porous Hugoniot values. There is no physical significance to the intercept value at zero particle velocity. A power function would provide a better fit to the low velocity points. The Hugoniots in the pressure - particle velocity plane are shown in Figure 5.

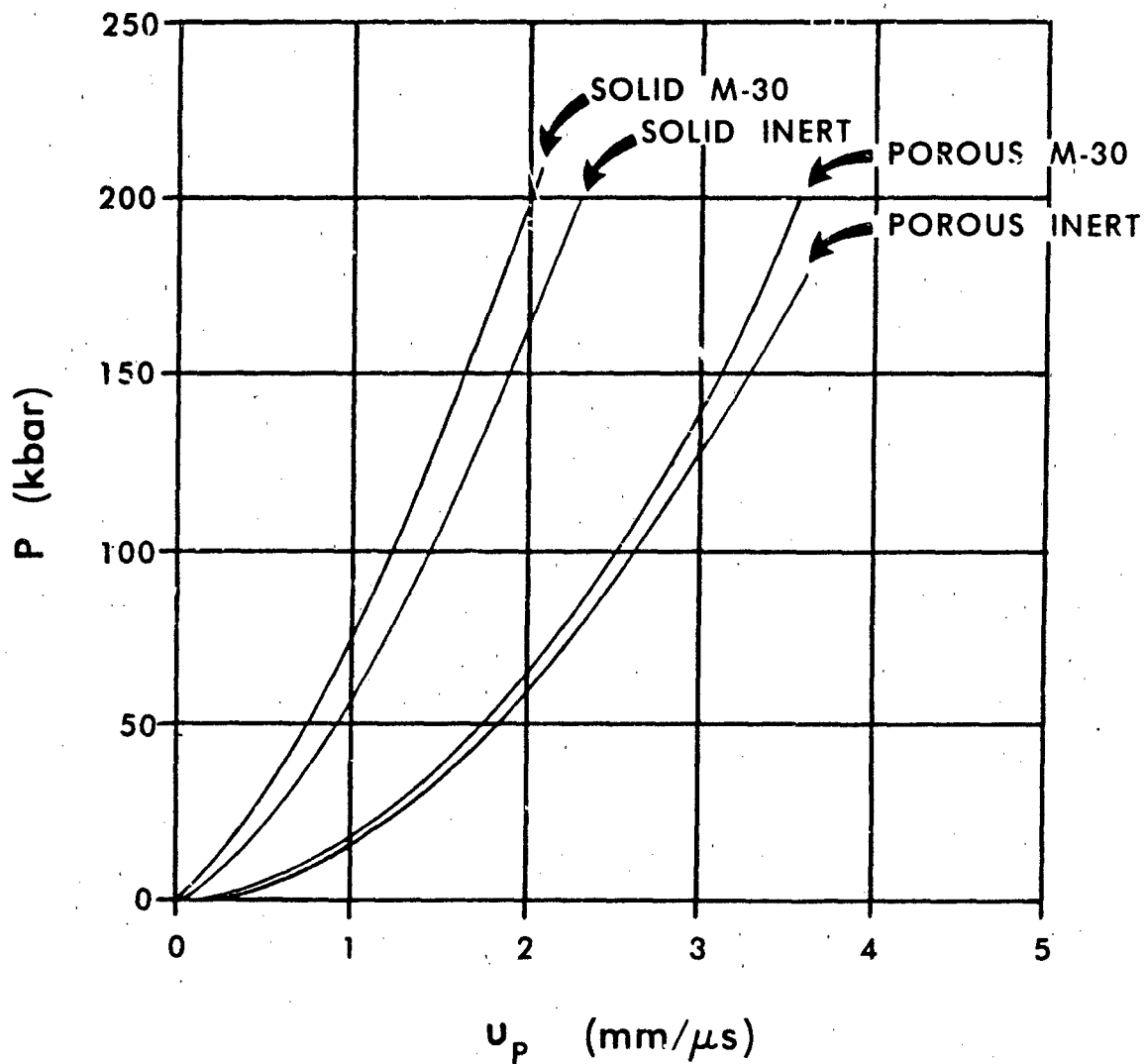


Figure 5. A Comparison of the Solid and Porous Hugoniot in the Pressure-Particle Velocity Plane.

V. DISCUSSION

The porous Hugoniot data allow one to calculate the pressure in the propellant bed due to shaped charge jet impact. This information is useful in performing hydrodynamic calculations for a non-reacting propellant bed. As shown in Table 1 the solid propellant undergoes violent reaction at an incident pressure of approximately 127 kbars, increasing to around 200 kbars within the measurement interval of one microsecond. However, it is anticipated that reaction could occur at lower pressures of longer duration, conditions which exist in the pressure field generated by jet impact. The solid Hugoniot reaction pressure may be a good way to, a priori, compare the response of various propellants upon shaped charge jet impact since impact pressures can be determined from known jet velocity and Hugoniot for the jet and propellant bed.

The question of the approach to mechanical equilibrium of porous samples is treated in reference 4. This reference used a one-dimensional Lagrangian computer program to simulate the response of powdered aluminum to a shock. The powdered aluminum was mocked up by a series of flat plates separated by gaps of width equal to the plate thickness. The calculated results were compared to experimental results on powdered aluminum and found to be in good agreement. The calculations showed an approach to equilibrium behind the shock for porous aluminum; the equilibrium states were consistent with the Rankine-Hugoniot jump conditions applied to the porous aluminum. The computational results indicated that the shock had to travel about ten times the plate thickness before mechanical equilibrium was established behind the shock wave.

The three-dimensional nature of a propellant bed would tend to promote a more rapid equilibration by the increased number of shock interactions per unit particle per unit time. On the other hand, "hot spots" would be produced in regions of convergent mass flow and because of the large grain size, these "hot spots" could persist over relatively long times. Therefore, the assumption of thermal equilibrium may not be strictly valid. Despite this limitation, it is believed that the porous Hugoniot calculated here are useful approximations to a real propellant bed.

REFERENCES

1. Rice, McQueen, Walsh, "Compression of Solids by Strong Shock Waves," Solid State Physics, Vol. 6, 1958.
2. Boyle, Smothers, Ervin, "The Shock Hugoniot of Unreacted Explosives," Fifth Symposium on Detonation, Aug. 18 - 21, 1970.
3. Herrmann, W., "Constitutive Equation for the Dynamic Compaction of Ductile Porous Materials," JAP, Vol. 40, No. 6, May 1969.
4. Hoffman, Andrews, Maxwell, "Computed Shock Response of Porous Aluminum," JAP, Vol. 39, No. 10, Sept. 1968.
5. Erkman, Edwards, "Computed and Experimental Hugoniots for Unreacted Porous High Explosives," Sixth Symposium on Detonation, Aug. 24 - 27, 1976.
6. Zeldovich, Raizer. "Physics of Shock Waves and High Temperature Hydrodynamic Phenomena," Vol. II, Academic Press, New York, 1967.

LIST OF SYMBOLS

SYMBOL

a	volume coefficient of thermal expansion
b	coefficient in the Hugoniot relationship, $U_s = b + su_p$
s	coefficient in the Hugoniot relationship, $U_s = b + su_p$
C_o	bulk sound velocity
C_p	specific heat at constant pressure
E	specific internal energy
E_f	specific internal energy of compressed porous material
E_{of}	initial specific internal energy of porous material
E_s	specific internal energy of compressed solid material
E_{os}	initial specific internal energy of solid material
G	Gruneisen constant
P	pressure
P_f	pressure in compressed porous material
P_{of}	initial pressure in porous material
P_s	pressure in compressed solid material
P_{os}	initial pressure in solid material
U_s	shock velocity
U_{sf}	shock velocity in porous material
u_p	particle velocity
u_{pf}	particle velocity in porous material
V	specific volume of compressed material
V_{of}	initial specific volume of porous material
V_{os}	initial specific volume of solid material
ρ	density of compressed material
ρ_{os}	initial density of solid material
ρ_{of}	initial density of porous material

DISTRIBUTION LIST

<u>No. of</u> <u>Copies</u>	<u>Organization</u>	<u>No. of</u> <u>Copies</u>	<u>Organization</u>
12	Administrator Defense Technical Info Center ATTN: DTIC-DDA Cameron Station Alexandria, VA 22304-6145	1	Commander Armament R&D Center US Army AMCCOM ATTN: SMCAR-LCE, Dr. N. Slagg Dover, NJ 07801
1	HQDA DAMA-ART-M Washington, DC 20310	1	Commander Armament R&D Center US Army AMCCOM ATTN: SMCAR-LCN, Dr. P. Harris Dover, NJ 07801
2	Chairman DOD Explosives Safety Board ATTN: Dr. T. Zaker COL O. Westry Room 856-C Hoffman Bldg 1 2461 Eisenhower Avenue Alexandria, VA 22331	1	Commander US Army Armament Materiel and Readiness Command ATTN: SMCAR-ESP-L Rock Island, IL 61299
1	Commander US Army Materiel Command ATTN: AMCDRA-ST 5001 Eisenhower Avenue Alexandria, VA 22333	1	Director Benet Weapons Laboratory US Army AMCCOM ATTN: SMCAR-LCB-TL Watervliet, NY 12189
1	Commander Armament R&D Center US Army AMCCOM ATTN: SMCAR-TSS Dover, NJ 07801	1	Commander US Army Aviation Research and Development Command ATTN: AMSAV-E 4300 Goodfellow Boulevard St. Louis, MO 63120
1	Commander Armament R&D Center US Army AMCCOM ATTN: SMCAR-LCE, Dr. R. F. Walker Dover, NJ 07801	1	Director US Army Air Mobility Research and Development Laboratory Ames Research Center Moffett Field, CA 94035
1	Air Force Armament Laboratory ATTN: AFATL/DLODL Eglin AFB, FL 32542-5000	1	Commander US Army Communications Electronics Command ATTN: AMSEL-ED Fort Monmouth, NJ 07703

DISTRIBUTION LIST

<u>No. of</u> <u>Copies</u>	<u>Organization</u>	<u>No. of</u> <u>Copies</u>	<u>Organization</u>
1	Commander ERADCOM Technical Library ATTN: DELSD-L(Reports Section) Frot Monmouth, NJ 07703-5301	1	Commander US Army Research Office ATTN: Chemistry Division P.O. Box 12211 Research Triangle Park, NC 27709
1	Commander US Army Missile Command ATTN: AMSMI-R Redstone Arsenal, AL 35809	1	Commander Office of Naval Research ATTN: Dr. J. Enig, Code 200B 800 N. Quincy Street Arlington, VA 22217
1	Commander US Army Missile Command ATTN: AMSMI-YDL Redstone Arsenal, AL 35809	1	Commander Naval Sea Systems Command ATTN: Mr. R. Beauregard, SEA 64E Washington, DC 20362
1	Commander US Army Missile Command ATTN: AMSME-RK, Dr. R.G. Rhoades Redstone Arsenal, AL 35809	1	Commander Naval Explosive Ordnance Disposal Facility ATTN: Technical Library Code 604 Indian Head, MD 20640
1	Commander US Army Tank Automotive Command ATTN: AMSTA-TSL Warren, MI 48090	1	Commander Naval Research Lab ATTN: Code 6100 Washington, DC 20375
1	Director US Army TRADOC Systems Analysis Activity ATTN: ATAA-SL White Sands Missile Range NM 88002	1	Commander Naval Surface Weapons Center ATTN: Code G13 Dahlgren, VA 22448
	Commandant US Army Infantry School ATTN: ATSH-CD-CSO-OR Fort Benning, GA 31905	9	Commander Naval Surface Weapons Center ATTN: Mr. L. Roslund, R122 Mr. M. Stosz, R121 Code X211, Lib E. Zimet, R13 R.R. Bernecker, R13 J.W. Forbes, R13 S.J. Jacobs, R10 Dr. C. Dickinson J. Short, R12 Silver Spring, MD 20910
1	Commander JS Army Development & Employment Agency ATTN: MODE-TED-SAB Fort Lewis, WA 98433		

DISTRIBUTION LIST

<u>No. of Copies</u>	<u>Organization</u>	<u>No. of Copies</u>	<u>Organization</u>
4	Commander Naval Weapons Center ATTN: Dr. L. Smith, Code 3205 Dr. A. Amster, Code 385 Dr. R. Reed, Jr., Code 388 Dr. K.J. Graham, Code 3835 China Lake, CA 93555	1	Director Sandia National Lab ATTN: Dr. J. Kennedy Albuquerque, NM 87185
			<u>Aberdeen Proving Ground</u>
1	Commander Naval Weapons Station NEDED ATTN: Dr. Louis Rothstein, Code 50 Yorktown, VA 23691		Dir, USAMSAA ATTN: AMXSJ-D AMXSJ-MP, H. Cohen Cdr, USATECOM ATTN: AMSTE-TO-F Cdr, CRDC, AMCCOM, ATTN: SMCCR-RSP-A SMCCR-MU SMCCR-SPS-IL
1	Commander Fleet Marine Force, Atlantic ATTN: G-4 (NSAP) Norfolk, VA 23511		
1	Commander Air Force Rocket Propulsion Laboratory ATTN: Mr. R. Geisler, Code AFRPL MKPA Edwards AFB, CA 93523		
1	AFWL/SUL Kirtland AFB, NM 87117		
1	Commander Ballistic Missile Defense Advanced Technology Center ATTN: Dr. David C. Sayles P.O. Box 1500 Huntsville, AL 35804		
1	Director Lawrence Livermore National Lab University of California ATTN: Dr. M. Finger P.O. Box 808 Livermore, CA 94550		
1	Director Los Alamos National Lab ATTN: John Ramsey P.O. Box 1663 Los Alamos, NM 87545		

USER EVALUATION SHEET/CHANGE OF ADDRESS

This Laboratory undertakes a continuing effort to improve the quality of the reports it publishes. Your comments/answers to the items/questions below will aid us in our efforts.

1. BRL Report Number _____ Date of Report _____
2. Date Report Received _____
3. Does this report satisfy a need? (Comment on purpose, related project, or other area of interest for which the report will be used.) _____

4. How specifically, is the report being used? (Information source, design data, procedure, source of ideas, etc.) _____

5. Has the information in this report led to any quantitative savings as far as man-hours or dollars saved, operating costs avoided or efficiencies achieved, etc? If so, please elaborate. _____

6. General Comments. What do you think should be changed to improve future reports? (Indicate changes to organization, technical content, format, etc.) _____

CURRENT ADDRESS

Name _____

Organization _____

Address _____

City, State, Zip _____

7. If indicating a Change of Address or Address Correction, please provide the New or Correct Address in Block 6 above and the Old or Incorrect address below.

OLD ADDRESS

Name _____

Organization _____

Address _____

City, State, Zip _____

(Remove this sheet along the perforation, fold as indicated, staple or tape closed, and mail.)